

Surface reflectance spectroscopy studies of chemisorption on W(100)*

J. Anderson[†]

Department of Physics, Brown University, Providence, Rhode Island 02912

G. W. Rubloff[‡]

IBM Thomas J. Watson Research Center, Yorktown Heights, New York 10598

M. A. Passler and P. J. Stiles

Department of Physics, Brown University, Providence, Rhode Island 02912

(Received 11 April 1974)

Surface reflectance spectroscopy (SRS) has been used to study chemisorption-induced changes in the electronic structure of a clean W(100) surface. The relative changes in optical reflectance, $\Delta R/R$, caused by chemisorption of H_2 , CO, and O_2 have been measured as a function of exposure and photon energy $\hbar\omega$ in the range $0.6 < \hbar\omega < 4.8$ eV for adatom coverages up to ≈ 1 monolayer. Structure in the exposure and coverage dependence of $\Delta R/R$ displays the various adatom binding states and also indicates the presence of adatom-adatom interactions within a given binding state. The model of McIntyre and Aspnes (MA) is adopted to relate the observed $\Delta R/R(\hbar\omega)$ to changes in an effective complex surface dielectric function $\Delta\hat{\epsilon}^s(\hbar\omega)$; by assuming a simple form for $\Delta\hat{\epsilon}^s(\hbar\omega)$, we fit $\Delta R/R(\hbar\omega)$ spectra calculated using the MA model to the experimental data and thereby obtain difference spectra $\Delta\hat{\epsilon}^s(\hbar\omega)$ which show the chemisorption-induced changes in the optical response of the surface region. The positions of prominent peaks and dips in $\Delta\epsilon_2^s (= \text{Im}\Delta\hat{\epsilon}^s)$ give the energies of important optical transitions associated with the surface electronic structure which are produced or quenched by chemisorption. These energies show a strong correlation with the position of surface levels (relative to the Fermi energy E_F) seen in ultraviolet photoemission and field-emission spectroscopies. As a result, the excitations obtained from SRS are attributed to optical transitions from intrinsic surface states and adsorbate-induced surface orbitals to final states concentrated primarily at E_F , which are most likely the tails of extended (Bloch) states of the metal as modified at the surface.

I. INTRODUCTION

The electronic structure of solid surfaces has recently become a subject of rapidly growing interest and effort, particularly with the application of electron spectroscopies to the study of chemisorption on atomically clean surfaces in ultrahigh vacuum (UHV). These techniques are inherently surface sensitive because the scattering length or escape depth of hot electrons in solids is short (5–20 Å), and as a result the hot electrons emerging from the sample originate mostly from the region near the surface. By far the greatest portion of spectroscopic information about the electronic structure of surfaces has come from those electron spectroscopies which measure essentially the density of filled electron states near the surface: ultraviolet photoemission (UPS),^{1–3} field-emission (FES),^{4,5} and ion-neutralization (INS)⁶ spectroscopies.

The spectrum of one-electron excitations of the surface electronic structure represents a valuable complement to the density of filled states near the surface since these excitations can provide important new information not accessible to UPS, FES, or INS: the empty final states to which electrons in the filled surface orbitals are excited, the energies of empty surface states, and the dielectric response of the surface electronic structure. The

energies of transitions associated with surface excitations have been determined in a few cases by electron-energy-loss measurements,^{7,8} but the results can be complicated by dynamic interference effects.⁸

Optical spectroscopy has been the primary method for measuring characteristic excitations in solids and has played an invaluable role in elucidating bulk electronic structure. Optical experiments have been considerably less important for surface studies because the relatively large penetration depth of light in solids (100–500 Å) makes these measurements rather insensitive to the properties of the surface. Nevertheless, very precise techniques of reflectance and modulation spectroscopy have been developed to extract fine details of the optical spectra for information on bulk properties, and the high sensitivity of these techniques makes it possible to study surface effects optically.

Differential reflectance measurements on metal surfaces in electrolyte solutions^{9,10} have demonstrated that optical experiments can provide useful information on the surface properties of optically absorbing solids. The complications of ionic double-layer and electroreflectance effects due to the applied electric field used in these studies underscore the desirability of carrying out optical measurements on atomically clean surfaces in UHV for studies of electronic surface orbitals associated

with chemisorption and intrinsic surface states present only on the clean surface. Optical absorption processes involving surface states on Ge and Si surfaces in UHV have been observed by a multiple total internal reflection technique,¹¹ but this method is restricted to photon energies $\hbar\omega$ below the fundamental absorption edge of semiconductors and insulators. Classical ellipsometry, normally carried out at a single wavelength, is well known to be sensitive to thin adsorbed films on surfaces and has been carried out for UHV chemisorption; the recent extension of ellipsometry to multiple wavelengths^{12,13} promises to yield spectroscopic information on surface electronic properties.¹⁴

We have previously demonstrated that high-precision optical techniques can detect relative changes $\Delta R/R$ in the near-normal incidence reflectance of an opaque substrate caused by chemisorption of small fractions ($\gtrsim \frac{1}{20}$) of a monolayer of adatoms on an atomically clean surface in UHV.^{15,16} By interpreting the differential reflectance spectra within the framework of a simple dielectric model, we obtain a surface reflectance spectroscopy (SRS) for UHV chemisorption which yields valuable spectroscopic information about optical excitations involving electronic surface orbitals.¹⁷ In particular, comparison of transition energies derived from SRS with the position of filled surface orbitals measured by UPS and FES permits an interpretation of the electron states involved in the transitions, as shown in a condensed account of our results for H₂ chemisorption on W(100).¹⁷

In the present paper we give a complete description of our SRS results for H₂, CO, and O₂ chemisorption on W(100) at room temperature. The dependence of $\Delta R/R$ on adatom coverage shows structure arising from the various sequential adatom binding states and indicates the presence of adatom-adatom interactions within a given binding state. Analysis of the spectral dependence of $\Delta R/R$ at fixed coverage yields optical transition energies which show a marked correlation with UPS and FES data. As a result, the transitions are identified as excitations from both intrinsic surface states of the clean surface and adsorbate-induced surface orbitals to empty final states at the Fermi energy E_F . In the case of simple gas chemisorption on W(100), therefore, the primary optical coupling of filled surface orbitals is to final states at E_F , which are probably the tails of extended (Bloch) states of the metal as modified at the surface, and no evidence yet exists for prominent empty surface orbitals.

II. EXPERIMENTAL TECHNIQUES

The single-crystal tungsten sample used in this investigation was in the form of a thin ribbon of dimensions $12 \times 3 \times 0.1$ mm with the surface oriented

to within $\frac{3}{4}^\circ$ of the (100) crystal plane. The sample was mechanically polished and then electropolished to achieve a smooth specular surface. This sample was one of several used in earlier low-energy-electron-diffraction (LEED) investigations,¹⁸ so a number of its properties with respect to adsorption of simple gases are well known. The surface was cleaned using procedures found adequate in the LEED experiments: it was resistively heated to $\sim 2100^\circ\text{C}$ in UHV for a brief period to remove adsorbates and was also periodically heated in O₂ to eliminate possible carbon contamination. The sample was held in stainless-steel clamps at each end under light spring tension to prevent buckling during heating. The sample temperature was monitored with a W-Re thermocouple spot-welded to the back surface of the ribbon near its midpoint. The reflectance changes were measured with a small focus of light at the middle of the sample.

The UHV chamber in which the sample was maintained had a base pressure of $\sim 5 \times 10^{-10}$ Torr, composed of roughly equal parts of H₂, CO, and argon. Adsorbate gases were admitted through leak valves at partial pressures of $\sim (1-2) \times 10^{-8}$ Torr and were monitored with a partial pressure analyzer. Thus the residual gases accounted for only a few percent of the total pressure during adsorption. During O₂ adsorption, however, the CO partial pressure rose to $\sim (1-2) \times 10^{-9}$ Torr or $\sim 10\%$ of the total.

The chemisorption-induced relative changes $\Delta R/R$ in near-normal ($\sim 5^\circ$) incidence reflectance were measured as a function of photon energy $\hbar\omega$ in the range $0.6 < \hbar\omega < 4.8$ eV and as a function of exposure e (= pressure \times time) corresponding to coverages θ up to the order of one monolayer. Light from a tungsten/halogen lamp ($\hbar\omega \leq 3$ eV) or a high-pressure xenon arc lamp ($\hbar\omega > 1.5$ eV) was dispersed by a fused quartz prism monochromator and focused to a spot of ~ 1 mm² on the sample through a sapphire window on the UHV chamber. The sample surface was tilted by $\sim 5^\circ$ from the window surface to spatially separate the reflections from the sample and the window. The photon energy resolution was typically 50 meV. Photomultiplier detectors (S-13 and ERMA III) were used for $\hbar\omega \gtrsim 1.4$ eV, while a PbS photoconductive detector was employed for $\hbar\omega \lesssim 1.4$ eV. The average values of $\Delta R/R$ near 1.4 eV obtained with the PbS cell matched the photomultiplier values at this energy to well within the experimental errors; this matching was further substantiated by test measurements with an S-1 photomultiplier down to 1.2 eV and the PbS cell extended up to ~ 1.6 eV.

Since the relative reflectance changes $\Delta R/R$ induced by chemisorption of ~ 1 monolayer of adatoms are small ($\sim 1\%$)^{15,16} and must be studied in detail to obtain spectral and coverage-dependent structure, a very sensitive optical technique is required.

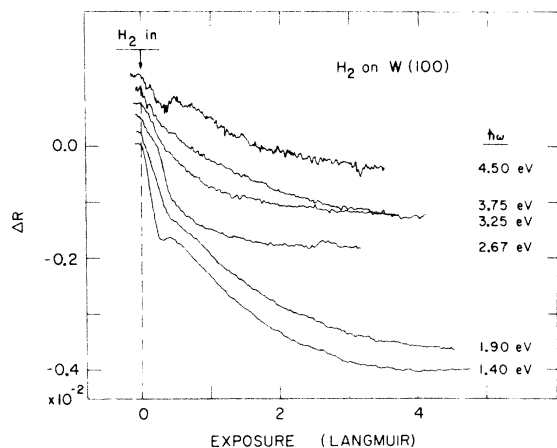


FIG. 1. Exposure dependence of reflectance changes for H_2 adsorption on W(100) at various photon energies.

We used a rotating-light-pipe scanning reflectometer¹⁹ which is capable of detecting changes in near-normal incidence reflectance at least as small as $|\Delta R/R| = 10^{-4}$. In this instrument a quartz light pipe, rotating at ~ 40 Hz, captures alternately the full reflected (RI_0) and incident (I_0) light beams and transmits them to the detector by total internal reflection. An electronic gating circuit, which uses field-effect transistors as switches for sample-and-hold measurements, extracts from the time-dependent signal the amplitudes of the RI_0 and I_0 beams averaged over their rather large duty cycles ($\sim 20\%$ of the period each). For photomultiplier detection, the reflectance $R = RI_0/I_0$ is directly obtained by keeping I_0 constant, using an operational amplifier power supply to vary the high voltage applied to the photomultiplier and thus to program its gain. In the usual application of the reflectometer, reflectance spectra $R(\hbar\omega)$ are then obtained by simply scanning $\hbar\omega$.

Since the change in surface properties caused by chemisorption does not alter the optical alignment, the full sensitivity of the reflectometer is available for surface studies. In the present surface studies, the sample was cleaned by heating, allowed to cool for 30–60 sec to within a few degrees of room temperature, and then at time $t=0$ it was exposed to the adsorbate gas at constant pressure p . By recording the reflectance R with time t , we obtained exposure curves $R(e)$ ($e = p \times t$) for various photon energies $\hbar\omega$. From these data both $\Delta R(e)$ at various $\hbar\omega$ and $\Delta R/R(\hbar\omega)$ at various e were deduced. This procedure was found to be more free of drift in determining $\Delta R/R(\hbar\omega, e)$ than measuring a sequence of $R(\hbar\omega)$ spectra after fixed doses of the adsorbate gas (exposure increments). Using the photomultiplier in favorable spectral regions, noise in the exposure curves is of the order of $\Delta R/R$

$= 10^{-4}$ [compared to total changes at monolayer coverage of $\Delta R/R = (0.5-1.0) \times 10^{-2}$], while the scatter in $\Delta R/R(\hbar\omega)$ at fixed e is typically a few $\times 10^{-4}$.

Weaker signals from the PbS detector used for $\hbar\omega < 1.4$ eV required longer integration times (~ 30 sec), which prevented continuous measurements of $\Delta R(e)$. However, the total change $\Delta R(e) = R(e) - R(0)$ was determined by measuring $R(0)$ and then $R(e)$ after a fixed exposure. These reflectance measurements were accomplished by accumulating the signal waveform for ~ 30 sec in a multichannel analyzer, averaging RI_0 and I_0 over the appropriate channels and taking the ratio RI_0/I_0 . In this mode the typical scatter for a set of identical measurements was $\sim 10^{-3}$.

III. RESULTS: EXPOSURE AND COVERAGE DEPENDENCE

Families of representative exposure curves $\Delta R(e)$ are shown in Figs. 1, 2, and 3 for H_2 , CO, and O_2 adsorption, respectively, for various photon energies in the range $\hbar\omega \geq 1.40$ eV, where photomultiplier detection was used. For clarity the curves are offset in the vertical direction as indicated by the $\Delta R = 0$ bars at left. After a brief resistance heating to ~ 2100 °C for cleaning the surface and a short time delay for cooling, the reflectance R was recorded as a function of time t for each $\hbar\omega$. At $t=0$ (exposure $e = pt = 0$) the adsorbate gas was admitted at fixed partial pressure p . Exposure values are given in langmuirs ($1 \text{ L} \equiv 10^{-6}$ Torr sec). In all three cases R decreases with increasing e by amounts as large as $\Delta R = -4 \times 10^{-3}$. Because R as measured through the window with reflection losses is about 0.4, the relative changes $\Delta R/R$ are as large as -10^{-2} , or -1% . Since this is of the order of the surface layer thickness di-

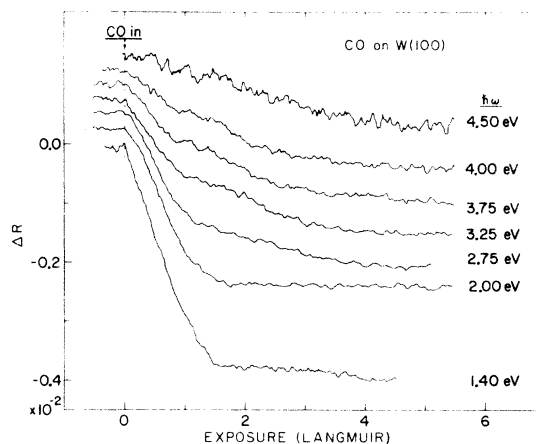


FIG. 2. Exposure dependence of reflectance changes for CO adsorption at various photon energies.

vided by the penetration depth of the light, we anticipate that chemisorption significantly alters the electronic structure of the surface.

The shape of the exposure curves $\Delta R(e)$ in Figs. 1–3 is roughly exponential, with ΔR saturating at exposures typical of those needed to produce a coverage of ~ 1 monolayer for these systems (approximately saturation). Distinct structure is present at certain low exposure values and alters the over-all exponential shape of the curves. This structure, in most cases, is associated with the sequential adsorption of adatoms into various binding configurations^{15,16} and is discussed in detail below. Both the structure and the total ΔR at saturation depend on photon energy.

Exclusive of adatom-adatom interactions, adatoms which bond to the surface in a given binding state should modify the local electronic structure near their bonding site in the same way. Thus the measured reflectance change ΔR per additional adatom should be constant within the exposure range where adsorption into a single binding state occurs. This behavior is expected independent of the explicit relation between the changes in surface electronic structure and the reflectance changes. At intermediate exposures the simultaneous presence of several different binding configurations may complicate this picture; furthermore, significant adatom-adatom interactions may even destroy the concept of characteristic adatom binding states, at least insofar as the electronic structure of the surface is concerned. To investigate the nature of adatom binding configurations, we convert the exposure curves $\Delta R(e)$ to coverage curves $\Delta R(\theta)$ (where coverage $\theta = 1.0$ represents an appropriately defined single adsorbed monolayer), using known sticking probabilities when available. In the absence of experimental data for $s(\theta)$, we assume the simplest behavior of the sticking probability, namely, that $s(\theta)$ depends only on the available surface area free of adatoms. Then $s(\theta)$ is linear in θ and is given by

$$s(\theta) = s_0(1 - \theta/\theta_s) \quad (1)$$

where s_0 is the initial sticking probability at $\theta = 0$ and θ_s is the saturation coverage in monolayers.

A. H₂ adsorption

A number of experiments indicate that H₂ adsorption on W(100) is dissociative and involves two binding states. Initially adatoms adsorb in the β_2 state, which gives a $c(2 \times 2)$ LEED pattern¹⁸ and a growth in the electron-stimulated-desorption (ESD) yield for H⁺ ions.²⁰ The intensities of both the $c(2 \times 2)$ LEED spots and the ESD cross section show a peak $\theta = 0.19$, where the distinct change in slope appears in $\Delta R(\theta)$ in Fig. 4. Near $\theta = 0.19$ formation of a second binding state β_1 begins¹⁸ and con-

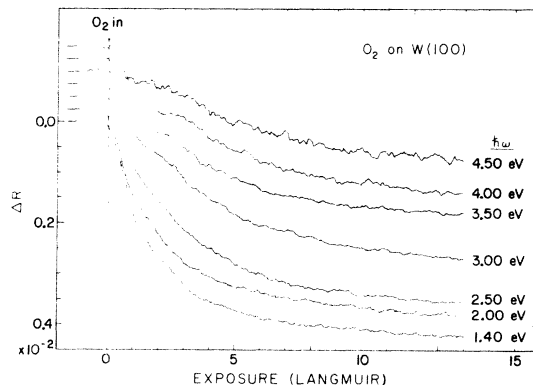


FIG. 3. Exposure dependence of reflectance changes for O₂ adsorption at various photon energies.

tinues to saturation, suppressing the ESD cross-section markedly²⁰ and causing the $c(2 \times 2)$ LEED spots to split.¹⁸ Flash-filament desorption measurements show two peaks corresponding to the β_1 and β_2 states,^{21,22} although recent results suggest that the distinct states seen in flash desorption may arise from a complex θ -dependent interaction.²⁰

Figure 4 shows coverage curves $\Delta R(\theta)$ for H₂ adsorption derived from the exposure curves of Fig. 1 using Madey's recent measurements²⁰ of $s(\theta)$. He found that Eq. (1) holds with $s_0 = 0.51$ and $\theta_s = 1.0$ monolayer = 2.0×10^{15} atoms/cm², or two H atoms per W surface atom. Structure is clearly evident in $\Delta R(\theta)$ at characteristic coverage values $\theta = 0.19$ and 0.26 for several curves, especially for $\hbar\omega = 1.40$ eV. These structures appear as fairly distinct changes in slope between three regions (labeled I, II, and III), each corresponding to a particular adatom binding configuration and having a nearly constant slope $S = d(\Delta R)/d\theta$. Since this slope varies with both $\hbar\omega$ and the coverage region, the reflectance change per additional adatom and thus the chemisorption-induced change in surface electronic structure both depend on adatom binding configuration as well as photon energy.

A two-binding-state picture of H₂ chemisorption on W(100) would give the following simple interpretation of, e.g., the $\Delta R(\theta)$ curve for $\hbar\omega = 1.40$ eV in Fig. 4. The constant slope S_I observed in region I gives the reflectance change per additional adatom for adsorption in the β_2 binding state as observed with light of energy $\hbar\omega = 1.40$ eV. The constant slope S_{III} in region III has a similar meaning but a different value ($S_{III} \neq S_I$) because adatoms adsorbed in the β_2 and β_1 states cause different changes in surface electronic structure. Adsorption in β_1 begins at $\theta = 0.19$. Field-emission studies have shown that as the β_1 state fills, the β_2 state is depleted.²³ Therefore, adatoms adsorbed in region II not only contribute with the β_1 slope S_{III} but make

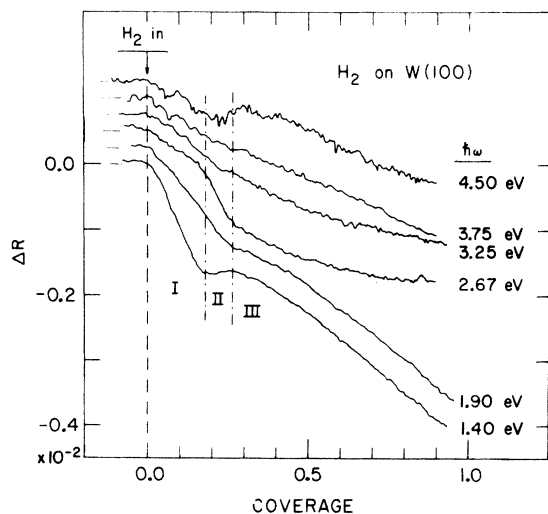


FIG. 4. Coverage dependence of reflectance changes for H_2 adsorption at various photon energies.

an additional contribution by converting adatoms previously in β_2 states to β_1 states. Since $S_I \cong 2S_{III}$, this conversion gives a positive contribution to S_{II} which is apparently large enough to make the net $S_{II} > 0$. The curves for large $\hbar\omega$ can also be explained in terms of these two effects.

However, for intermediate photon energies (2.67 and 3.25 eV) the slope in region II is steeper than that in regions I or II, and no combination of S_I and S_{III} can produce the observed S_{II} . Furthermore, if at large θ all adatoms already on the surface were in the β_1 state and further adatoms also went into the β_1 state, all curves near large θ should extrapolate back to $\Delta R = 0$ at $\theta = 0$, contrary to the observations for $\hbar\omega = 2.67$ and 3.25 eV. These results imply that a more complicated adsorption pattern takes place after $\theta = 0.19$, involving at least a third binding configuration or more likely a continuous change in binding configuration with coverage^{18,24} so that no single well-defined binding "state" exists after $\theta = 0.19$,¹⁷ at least from the point of view of surface electronic structure. Strong evidence for coverage-dependent chemisorption bonding and adatom-adatom interactions also comes from photoemission results which show structures in the density of filled states shifting in energy with θ after $\theta = 0.19$.²⁵⁻²⁷

B. CO adsorption

At room temperature and above, CO adsorbs on the W(100) surface in a series of tightly bound β states^{28,29} for coverage up to a monolayer. At higher exposures the CO occupies more weakly bound α states^{29,30} which desorb in the neighborhood of (300-400) °K. The bulk of evidence indicates that during room-temperature chemisorption

up to a monolayer, the CO layer is homogeneous, with only one β binding state populated, and that other β states observed during flash filament desorption arise as a result of thermal conversion. Although published values for the sticking coefficient $s(\theta)$ vary, there is general agreement that the β states are essentially saturated at an exposure of 4-6 L. Since the saturation coverage is 1×10^{15} molecules/cm²,²⁸ a linear $s(\theta)$ requires $s_0 \cong 1$. We therefore assume $s_0 = 1.0$ and $\theta_s = 1.0$ in Eq. (1), although we do not draw any conclusions that depend critically on a precise evaluation of intermediate coverage values.

The resulting coverage curves for CO adsorption are shown in Fig. 5. A pronounced structure appears at $\theta = 0.44$, corresponding to a similar feature in the exposure curves at $e = 1.4$ L (Fig. 2). At low $\hbar\omega$ this structure in $\Delta R(\theta)$ is particularly pronounced and consists of a distinct change in slope between linear segments. Above $\theta = 0.44$ for $\hbar\omega \leq 2.00$ eV the slope is essentially zero, indicating that adsorption above the initial half monolayer does not affect the optical properties of the surface region; this produces the unusual shape of the exposure curves (Fig. 2) at low $\hbar\omega$, which are not at all exponential and give the impression that the adsorption saturates at smaller exposure values than those indicated by the data at larger $\hbar\omega$. The discontinuity in slope of $\Delta R(\theta)$ near a half monolayer suggests that the physical properties of the first and second half-monolayers may differ; however, except for a local inflection in work function³¹ and a possible change in sticking coefficients,²⁸ there is no other experimental evidence for such a change in properties at half a monolayer. We believe it more likely, as discussed in more detail below, that the

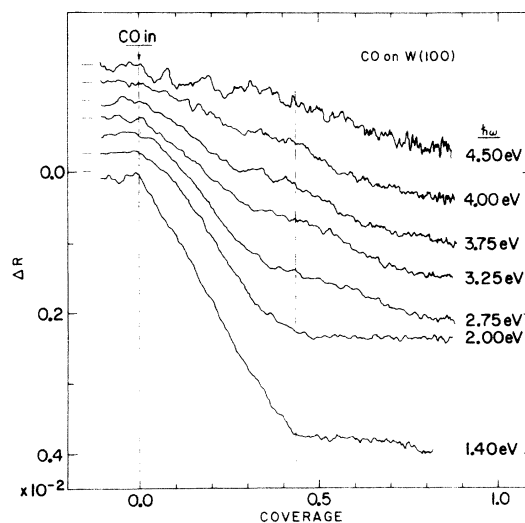


FIG. 5. Coverage dependence of reflectance changes for CO adsorption at various photon energies.

structure near a half monolayer is associated with changes in the surface electronic structure which are essentially unrelated to and unaccompanied by changes in the adsorbate binding configuration.

C. O₂ adsorption

Detailed measurements of the sticking probability for O₂ adsorption on W(100) have been reported by Madey. He found $s_0 \cong 1.0$ and that at monolayer coverage ($\theta = 1.0 = 10^{15}$ atoms/cm²) $s \cong 0.15$, giving a saturation coverage of somewhat more than a monolayer. Although some weak reproducible structure in $s(\theta)$ was found, $s(\theta)$ is nearly linear and extrapolates to a saturation coverage $\theta_s \cong 1.2$. Figure 6 shows coverage curves for O₂ adsorption calculated from Eq. (1) with $s_0 = 1.0$ and $\theta_s = 1.2$. Structure near one-half monolayer coverage is indicated, and $\Delta R(\theta)$ is not linear on either side of this point. It appears that corrections to $\Delta R(\theta)$ to take into account the reported deviations of $s(\theta)$ from linearity³² would not produce straight line segments in $\Delta R(\theta)$ but would enhance the nonlinearities. The coverage curves also show a different behavior above $\theta = 1.0$, particularly for large $\hbar\omega$, where a change in slope at $\theta = 1.0$ is apparent.

The adsorption features displayed in the coverage curves (Fig. 6) are consistent with other measurements. The structure near $\theta = 0.5$ is apparently related to the β_2 adsorption state, which gives near $\theta = 0.5$ a maximum O⁺ yield in ESD,³² a maximum intensity of a 4×1 LEED pattern,³³ and an inflection point in the work-function-change versus θ curve.³² Below $\theta = 1.0$, atomic oxygen is thermally desorbed,³⁴ while oxygen adsorbed above $\theta = 1.0$ gives a large O⁺ ESD yield (β_1 states)³² and desorbs as tungsten oxides³⁴; this suggests that the fraction-

al second monolayer is different in nature from the first monolayer, as indicated by the structure in $\Delta R(\theta)$ at $\theta = 1.0$.

Finally, LEED measurements have shown that the initial binding configurations for both CO and O₂ adsorption at room temperature (unordered for CO and ordered 4×1 for O₂) convert to ordered $c(2 \times 2)$ states after heating (to 1000 and 1300 °K, respectively).^{28,33} However, we found no measurable reflectance change after carrying out this conversion for an adsorbed half-monolayer of CO or O₂. This result is consistent with photoemission experiments which show only very minor changes in the energy distribution curves due to interconversion between CO binding states.³⁵ These observations suggest that in some cases the reordering of adatom binding structure seen in LEED does not involve significant changes in surface electronic structure, probably because the bonding of primary importance—that between adatom and surface atoms in a surface molecular complex—is essentially the same for the original and converted binding configurations.

The structure observed in the exposure and coverage curves show clearly that surface reflectance spectroscopy can be a sensitive probe of the adsorption state and its kinetics as far as the fundamental chemisorption bonding is concerned. This is because SRS, as an optical technique, measures chemisorption-induced changes in the electronic properties of the surface. Thus a change in adatom binding configuration which involves a considerable modification of the chemisorption bond will produce a change in the reflectance change per additional adatom and lead to structures in $\Delta R(e)$ and $\Delta R(\theta)$, as observed.

IV. RESULTS: SPECTRAL DEPENDENCE

The fundamental electronic structure information gained from optical measurements comes from the spectral dependence of the optical response, which indicates the characteristic energies of prominent excitations, the joint density of states, and relative oscillator strengths of excitations of the electronic structure. For a given type of chemisorption bond associated with a certain adatom binding configuration, spectroscopic information is already contained in the $\Delta R(\theta)$ curves as the variation in slope $d(\Delta R)/d\theta$ with photon energy $\hbar\omega$. However this spectral dependence is more clearly displayed by plotting $\Delta R/R(\hbar\omega)$ at certain coverage values corresponding to characteristic states of adsorption (which determine the surface electronic structure). Such spectral curves were constructed from numerous exposure and coverage curves taken over the range $1.4 < \hbar\omega < 4.8$ eV using photomultiplier detection and were supplemented by measurements of $\Delta R/R$ at fixed θ obtained in the range $0.6 < \hbar\omega < 1.5$ eV with a PbS detector as described in Sec.

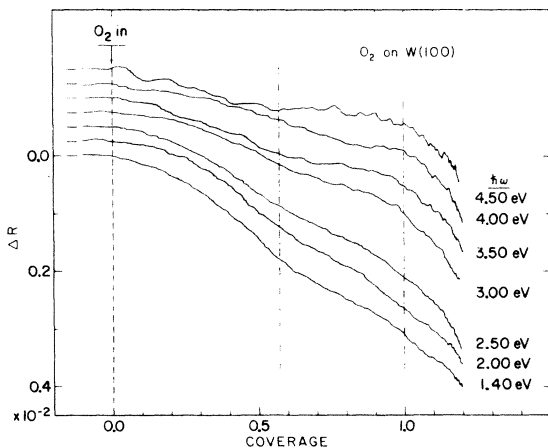


FIG. 6. Coverage dependence of reflectance changes for O₂ adsorption at various photon energies.

II.

The resulting spectral curves $\Delta R/R(\hbar\omega)$ for H_2 , CO, and O_2 adsorption are shown by the data points in Figs. 7, 8, and 9, respectively. As mentioned previously, $\Delta R/R$ is negative above 1.4 eV and is as large as about 1% (10^{-2}) at saturation. In all three cases $\Delta R/R$ increases to positive values with decreasing $\hbar\omega$ below ~ 1.5 eV. For H_2 and CO adsorption the $\Delta R/R$ values below ~ 1.2 eV are essentially the same at the fractional coverage shown in Figs. 7 and 8 as at saturation; this indicates that for low $\hbar\omega$ no further significant changes in reflectance (and therefore in surface electronic structure) take place after $\theta = 0.19$ for H_2 adsorption and after $\theta = 0.44$ for CO adsorption. The similarity of $\Delta R/R(\hbar\omega)$ below 1.2 eV for all three adsorbates suggests that the strong structure at low $\hbar\omega$ is a common feature of chemisorption on W(100) independent of the identity of the particular adsorbate.

In contrast, various structures appear in the spectral curves above ~ 1.5 eV which change with the adsorbate. In the H_2 spectra in Fig. 7 the $\theta = 0.19$ and $\theta = 1.00$ curves represent reflectance changes associated with adsorption in the initial β_2 state and at the saturation coverage of one monolayer, respectively. At $\theta = 1.00$ a peak near 3.1 eV and dips near 2.0 and 4.2 eV show up clearly. Structure also seems to appear for $\theta = 0.19$, e.g., near 1.6 eV, but it is more difficult to assess because the total $\Delta R/R$ is smaller at lower θ and hence the signal/noise ratio is smaller.

The $\Delta R/R(\hbar\omega)$ spectra for CO (Fig. 8) are rela-

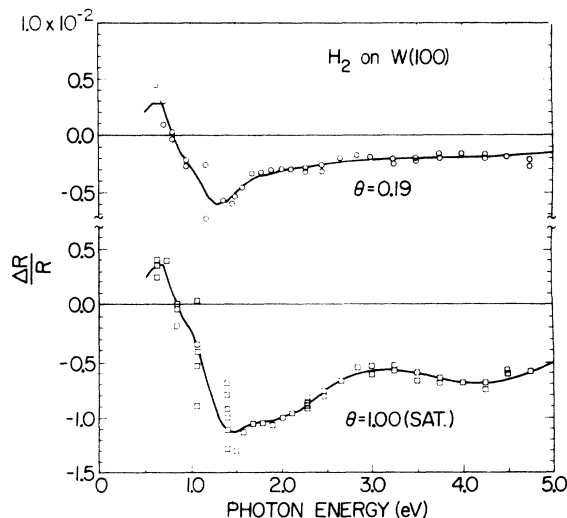


FIG. 7. Spectral dependence of relative reflectance changes for H_2 adsorption at coverages $\theta = 0.19$ and $\theta = 1.00$ (saturated surface). Points, experimental data; solid curves, results of a theoretical fit to the data as described in text.

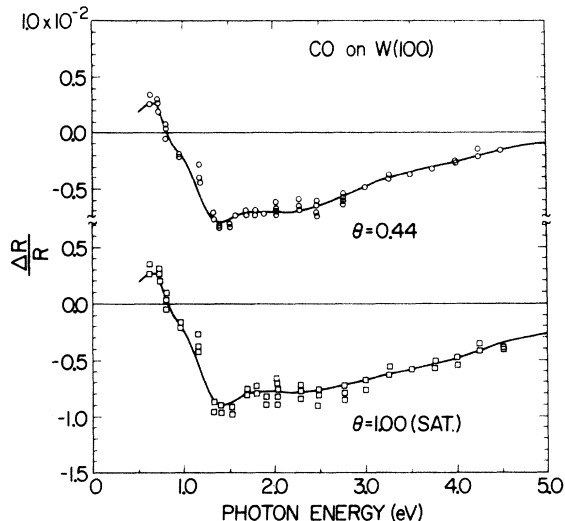


FIG. 8. Spectral dependence of relative reflectance changes for CO adsorption at coverages $\theta = 0.44$ and $\theta = 1.00$ (saturated surface). Points, experimental data; solid curves, theoretical fit to the data.

tively flat near 2 eV and rise gradually above 3 eV. They differ in shape from the H_2 spectra and have somewhat less pronounced structure above 2 eV. The CO spectra for $\theta = 0.44$ and $\theta = 1.00$ are quite similar in shape and have essentially identical $\Delta R/R$ values below ~ 2 eV, as noted in the lack of further reflectance changes above $\theta = 0.44$ in the coverage curves (Fig. 5) at low $\hbar\omega$. At higher $\hbar\omega$ the amplitude of $\Delta R/R$ for $\theta = 1.00$ becomes about twice that for $\theta = 0.44$. We regard this additivity of the reflectance change per adsorbed molecule as evidence for the homogeneity of the adsorbed layer, i.e., a single binding state, as seen at the higher photon energies.

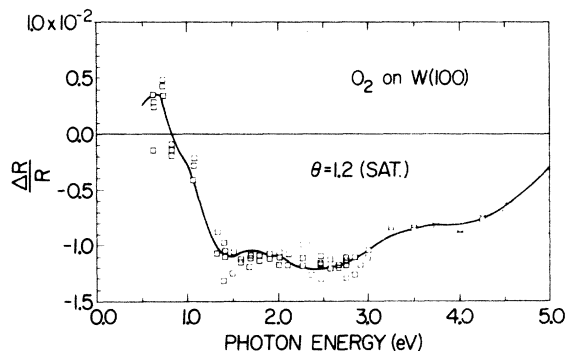


FIG. 9. Spectral dependence of relative reflectance changes for O_2 adsorption at saturation coverage ($\theta = 1.2$). Points, experimental data; solid curves, theoretical fit to the data.

Because of the complexity of the O₂ adsorption process as indicated by the nonlinear coverage curves (Fig. 6), the saturation at somewhat more than one monolayer,³² and the formation of oxides as seen in desorption products,³⁴ we analyze the spectral distribution of $\Delta R/R$ only for the saturated surface (Fig. 9). The structure, different from the H₂ and CO spectra, includes a shoulder near 3.1 eV and a further rise near 4.3 eV.

V. DIELECTRIC MODEL

The spectral features observed in $\Delta R/R(\hbar\omega)$ at low $\hbar\omega$ are independent of the identity of the particular adsorbate, while the energy position and shape of structures at higher $\hbar\omega$ show a noticeable dependence on the adsorbate species. An interpretation of the $\Delta R/R(\hbar\omega)$ spectra in terms of the electronic properties of the surface region might be made on the basis of the position of spectral features and their dependence on adsorbate identity and coverage. However, a more meaningful analysis requires a dielectric model to relate the observed reflectance changes to the chemisorption-induced changes in the surface electronic structure. Such a model would define the parameters used to characterize the actual dielectric response of electrons near the surface and prescribe the explicit relation between these parameters and the observed $\Delta R/R$. One could then determine the energies of prominent optical excitations associated with the surface electronic structure, which as a consequence of the Kramers-Kronig relations are given only approximately by the position of structures in $\Delta R/R(\hbar\omega)$, and as a result gain significant insight into the changes in surface electronic structure accompanying chemisorption.

As the simplest physical description of the surface dielectric response and its relation to the observed reflectance changes, we adopt the model of McIntyre and Aspnes (MA),³⁶ in which the surface region is treated as a uniform layer of (sub)monolayer thickness d_a ($\ll \lambda$, the wavelength of light) having complex dielectric function $\hat{\epsilon}^a(\omega) = \epsilon_1^a(\omega) + i\epsilon_2^a(\omega)$. This function is regarded as an effective response function which represents a local complex dielectric function $\hat{\epsilon}^a(z)$ (z normal to surface) averaged over the thickness d of the surface region. Structure in $\epsilon_2^a(\omega)$ is then taken as representing features of the joint density of states weighted by electric dipole matrix element effects, as in the case of bulk optical properties. For submonolayer films of reasonable adatom concentration, the adatom-adatom separation is small compared to λ and the film can be regarded as optically uniform with effective thickness d_a proportional to coverage.³⁶ Adsorption of such a film onto a bulk substrate having complex dielectric function $\hat{\epsilon}^b(\omega) = \epsilon_1^b(\omega) + i\epsilon_2^b(\omega)$ then produces a relative change in

near-normal incidence reflectance given by³⁶

$$\frac{\Delta R_a}{R} = -\frac{8\pi d_a}{\lambda} \left(\frac{\epsilon_2^b(\epsilon_1^a - \epsilon_1^b) - (\epsilon_1^b - 1)(\epsilon_2^a - \epsilon_2^b)}{(\epsilon_1^b - 1)^2 + (\epsilon_2^b)^2} \right), \quad (2)$$

or more simply

$$\frac{\Delta R_a}{R} = -\frac{8\pi d_a}{\lambda} \left(\frac{\epsilon_2^b(\epsilon_1^a - 1) - (\epsilon_1^b - 1)(\epsilon_2^a)}{(\epsilon_1^b - 1)^2 + (\epsilon_2^b)^2} \right). \quad (3)$$

Since the clean W(100) surface is known to have significant intrinsic surface states which are quenched by adsorption,²⁻⁴ it is important to incorporate these effects into the dielectric model. Intuitively we expect that just as adsorption produces new surface optical transitions which contribute to $\hat{\epsilon}^a$, so adsorbate-induced quenching of transitions involving intrinsic surface states should add a term to $\hat{\epsilon}^a$ having opposite sign. This can be shown in the following manner. The existence of intrinsic surface states produces a surface region of thickness d_i on the clean surface with electronic structure different from that of the underlying bulk. If one imagines this surface layer to be added on top of the bulk (as with the adsorbed layer case), it alters the reflectance (relative to that for the bulk without surface states) by

$$\frac{\Delta R_i}{R} = -\frac{8\pi d_i}{\lambda} \left(\frac{\epsilon_2^b(\epsilon_1^i - 1) - (\epsilon_1^b - 1)(\epsilon_2^i)}{(\epsilon_1^b - 1)^2 + (\epsilon_2^b)^2} \right), \quad (4)$$

where $\hat{\epsilon}^i(\omega)$ is the complex dielectric function of this surface region for the clean surface. Because the reflectance changes within the MA model are linear in the dielectric function of the surface layer, the total relative reflectance change $\Delta R/R$ is the sum of two contributions: (i) $-\Delta R_i/R$ due to adsorbate-induced quenching of optical transitions involving intrinsic surface states; and (ii) $\Delta R_a/R$ due to the production of new transitions involving adsorbate-induced surface orbitals. From Eqs. (3) and (4), $\Delta R/R = \Delta R_a/R - \Delta R_i/R$ becomes

$$\frac{\Delta R}{R} = -\frac{8\pi d_a}{\lambda} \left(\frac{\epsilon_2^b[\epsilon_1^a - f\epsilon_1^i - (1-f)] - (\epsilon_1^b - 1)(\epsilon_2^a - f\epsilon_2^i)}{(\epsilon_1^b - 1)^2 + (\epsilon_2^b)^2} \right), \quad (5)$$

where $f \equiv d_i/d_a$. We now define $\Delta\hat{\epsilon}^s = \Delta\epsilon_1^s + i\Delta\epsilon_2^s$ as the complex dielectric function of the surface region with real and imaginary components, respectively, given by

$$\Delta\epsilon_1^s \equiv \epsilon_1^a - f\epsilon_1^i - (1-f), \quad (6a)$$

$$\Delta\epsilon_2^s \equiv \epsilon_2^a - f\epsilon_2^i \quad (6b)$$

so that the reflectance change (5) becomes

$$\frac{\Delta R}{R} = -\frac{8\pi d_a}{\lambda} \left(\frac{\epsilon_2^b \Delta\epsilon_1^s - (\epsilon_1^b - 1) \Delta\epsilon_2^s}{(\epsilon_1^b - 1)^2 + (\epsilon_2^b)^2} \right). \quad (7)$$

This form is essentially identical to that given by McIntyre^{9,10} for electroreflectance effects due to modulation of the dielectric response of the surface region by the electric field at the metal sur-

face in an electrochemical cell. More generally, d_i and d_a in the above would be replaced by Δd_i and Δd_a to account for reflectance changes between different adatom coverage states of the surface.

Equation (7) relates the relative reflectance changes to changes in an average effective complex surface dielectric function which we would like to determine. The term in brackets has the form $\alpha\Delta\epsilon_1^s + \beta\Delta\epsilon_2^s$, where the coefficients α and β depend only on the bulk optical properties of the substrate. We have calculated these coefficients over the photon energy range of the measurements from the reported optical constants of tungsten.³⁷ Because of the short screening length ($\sim 0.5 \text{ \AA}$) of electrons in a metal, changes in electronic structure due to chemisorption do not penetrate into the substrate much further than the chemisorption bond, i. e., a few \AA . Although d_i and d_a for the clean and saturated surfaces need not be identical, we can assume $d_i = d_a$ ($f=1$) without serious error in the position and shape of structures in $\Delta\hat{\epsilon}^s(\hbar\omega)$. For if $f \neq 1$, then from Eq. (6) the relative strength of structures in $\hat{\epsilon}^a$ and $\hat{\epsilon}^i$ is somewhat altered, and $\Delta\epsilon_1^s$ is shifted down by a constant amount $(1-f)$; the significance of the position of structures in $\Delta\hat{\epsilon}^s$ remains. In the following analysis we assume $d_a \propto \theta$ and that for all adsorbates at saturation coverage $d_a = 5 \text{ \AA} = d_i$.

Because only one quantity, $\Delta R/R$, in Eq. (7) is measured, the two remaining unknowns $\Delta\epsilon_1^s$ and $\Delta\epsilon_2^s$ cannot be determined directly. This is a familiar problem for normal-incidence reflectance studies of bulk optical properties, where the usual procedure is to measure the reflectance over as broad a photon energy range as possible, choose some reasonable extrapolation outside the region of measurement, and calculate the reflectance phase angle and the optical constants by Kramers-Kronig analysis. However, the photon energy range covered in the present work is rather limited in comparison with many studies of bulk optical properties where Kramers-Kronig analysis was done, and the proper extrapolation of $\Delta R/R$ outside the range of measurement is not clear.

An alternative method to determine $\Delta\epsilon_1^s(\hbar\omega)$ and $\Delta\epsilon_2^s(\hbar\omega)$ from the measured $\Delta R/R(\hbar\omega)$ spectrum is to assume a simple form for $\Delta\hat{\epsilon}^s(\hbar\omega)$ and adjust its parameters to produce an optimum fit to the experimental data. By prescribing an algebraic relation between the two unknowns $\Delta\epsilon_1^s$ and $\Delta\epsilon_2^s$, this effectively reduces the problem to simply determining one unknown from one measurement. Such a procedure has been successfully used³⁸ to determine the optical constants $\epsilon_1(\hbar\omega)$ and $\epsilon_2(\hbar\omega)$ from normal-incidence reflectance data for bulk crystals, where $\hat{\epsilon}(\hbar\omega)$ was assumed to be composed of a few Lorentzian oscillators. This technique was found to be efficient and accurate and to pro-

duce good agreement with results obtained by Kramers-Kronig analysis. Therefore, although optical structures characteristic of the bulk electronic response are not expected to have Lorentzian shapes, this simple analytic form in practice provides a reasonably good picture of the spectral dependence of the optical constants and particularly the energy position of peaks and valleys in $\hat{\epsilon}(\hbar\omega)$. This makes the oscillator analysis especially attractive for determining from the $\Delta R/R(\hbar\omega)$ spectra the energies of prominent surface optical transitions. Furthermore, optical structures associated with the surface may be considerably better represented by a simple oscillator form than are bulk structures because (i) the Anderson model³⁹ as applied to chemisorption⁴⁰ predicts a Lorentzian density of states for virtual bound states produced by discrete adatom orbitals; (ii) in a similar way discrete orbitals of the molecular complex⁴¹ formed by bonding between the adatoms and surface metal atoms should be broadened into approximately symmetric resonances by interaction with the bulk metal; and (iii) for an ordered surface region, critical-point singularities in the joint density of states associated with the two-dimensional band structure appear as logarithmic divergences, which can be reasonably well described by Lorentzian line shapes. We emphasize, however, that the Lorentzian oscillator model used for $\Delta\hat{\epsilon}^s(\hbar\omega)$ is chosen primarily because of its simple form which guarantees that the real and imaginary components satisfy the Kramers-Kronig relations. No particular physical significance is attached to the optimum values of the oscillator parameters themselves, but only to the energy position (and to a somewhat smaller extent the relative magnitudes) of structures in the total $\Delta\hat{\epsilon}^s(\hbar\omega)$ spectra so derived.

We therefore assume that $\Delta\hat{\epsilon}^s$, the change in complex surface dielectric function within the MA model, is composed of a few Lorentzian oscillators

$$\Delta\hat{\epsilon}^s(\omega) = \Delta\epsilon_{bkg}^s + \sum_j \frac{A_j}{(\omega_j^2 - \omega^2) - i\Gamma_j\omega}, \quad (8)$$

so that $\Delta\hat{\epsilon}^s$ has real and imaginary components

$$\Delta\epsilon_1^s(\omega) = \Delta\epsilon_{bkg}^s + \sum_j \frac{A_j(\omega_j^2 - \omega^2)}{(\omega_j^2 - \omega^2)^2 + \omega^2\Gamma_j^2}, \quad (9a)$$

$$\Delta\epsilon_2^s(\omega) = \sum_j \frac{A_j\Gamma_j\omega}{(\omega_j^2 - \omega^2)^2 + \omega^2\Gamma_j^2}. \quad (9b)$$

Both positive and negative values of A_j are allowed in order to describe, respectively, the production of new transitions associated with chemisorption and the quenching of intrinsic surface state transitions by adsorption. According to the Kramers-Kronig relations, changes in surface optical absorption bands ($\Delta\epsilon_2^s$) outside the measured photon energy range will produce a nearly constant change

in dispersion $\Delta\epsilon_1^s$ within that range. Therefore, a real constant $\Delta\epsilon_{bkg}^s$ is added to the Lorentzian sum in Eq. (9) to account for this change in dispersion as well as the $1-f$ term in Eq. (6a), which is independent of $\hbar\omega$ but depends on the change in coverage which produces the observed $\Delta R/R$. With this model change in surface dielectric function, a theoretical $\Delta R/R(\hbar\omega)$ spectrum is then calculated within the framework of the MA model by Eq. (7). The parameters A_j , Γ_j , ω_j , and $\Delta\epsilon_{bkg}^s$ were adjusted by computer to obtain optimum fits of the theoretical $\Delta R/R(\hbar\omega)$ spectra to the experimental data. The results of this fit are shown by the solid curves in Figs. 7-9.

The imaginary part of the change in surface dielectric function as determined by the above procedure is shown in Figs. 10, 11, and 12 for H_2 , CO, and O_2 adsorption, respectively. The positions of extrema in the $\Delta\epsilon_2^s(\hbar\omega)$ spectra are determined to about ± 0.2 and ± 0.4 eV for the structures above and below ~ 1.5 eV, and the structures are typically 1.5-2.5 eV wide. A strong dip in $\Delta\epsilon_2^s$ at low $\hbar\omega$ dominates all these spectra, while weaker structures which differ for the different adsorbates appear at higher $\hbar\omega$. The large magnitude of $\Delta\epsilon_2^s$ at low $\hbar\omega$ is expected because the coefficients in Eq. (7) are considerably smaller in this region compared with the higher $\hbar\omega$ range even though the $\Delta R/R$ magnitudes are comparable. We also note that since bulk tungsten has $\epsilon_2^b \geq 10(\epsilon_1^b - 1)$ above 2 eV and the magnitudes of $\Delta\epsilon_1^s$ and $\Delta\epsilon_2^s$ are comparable for a Lorentzian oscillator, the $\Delta R/R(\hbar\omega)$ spectrum above 2 eV is proportional to $-\Delta\epsilon_1^s(\hbar\omega)$. This provides a simple check of the fitting procedure: for O_2 adsorption (Fig. 9) the S-shaped resonance centered near 3.2 eV in $\Delta R/R(\hbar\omega)$, consisting of a dip below and a peak above the center en-

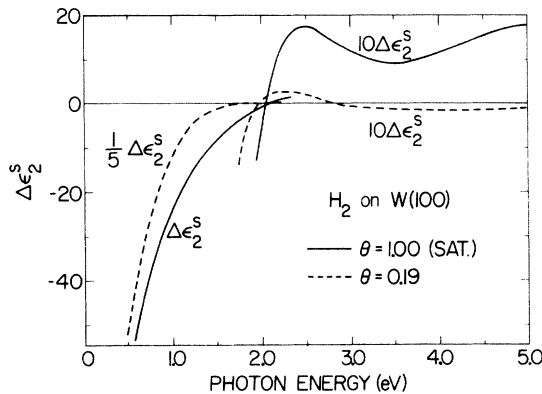


FIG. 10. Spectral dependence of the change in imaginary part of the surface dielectric function for H_2 adsorption at coverages $\theta = 0.19$ and $\theta = 1.00$. The model used to obtain $\Delta\epsilon_2^s(\hbar\omega)$ from the $\Delta R/R(\hbar\omega)$ data is described in text.

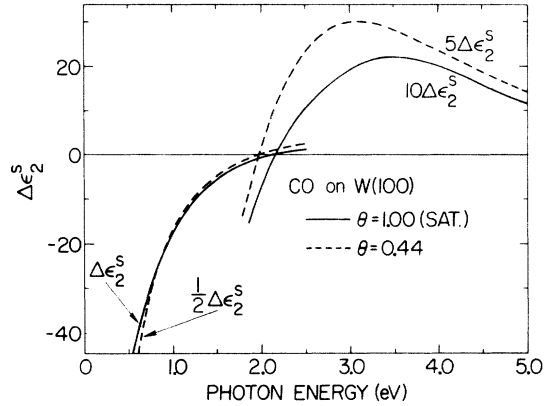


FIG. 11. Spectral dependence of the change in imaginary part of the surface dielectric function for CO adsorption at coverages $\theta = 0.44$ and $\theta = 1.00$.

ergy, resembles $-\Delta\epsilon_1^s(\hbar\omega)$, where $\Delta\epsilon_1^s(\hbar\omega)$ is the real part of a Lorentzian structure at the same energy. The corresponding imaginary part $\Delta\epsilon_2^s(\hbar\omega)$ produces the peak seen in Fig. 12 at 3.2 eV.

VI. DISCUSSION

The above dielectric model gives a simple prescription for determining the change in surface dielectric response from the measured reflectance changes. It also indicates how the structures in the resulting $\Delta\hat{\epsilon}^s(\omega)$ spectra can be interpreted in terms of surface optical transitions involving new adsorbate-induced orbitals associated with the chemisorption bond ($A_j > 0$) and intrinsic surface states of the clean surface which are quenched by adsorption ($A_j < 0$). However, the changes in surface dielectric response could in principle be due in part to chemisorption-induced changes in the strength of bulk transitions ($\sim \hat{\epsilon}^b$) within the surface

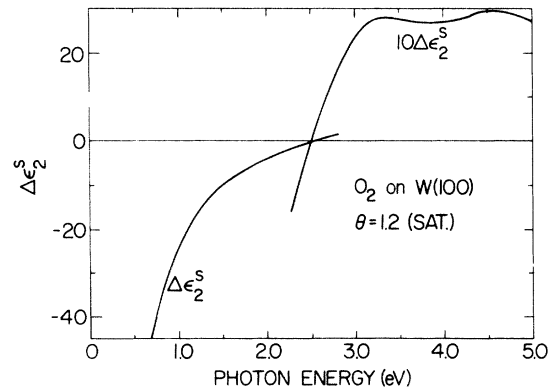


FIG. 12. Spectral dependence of the change in imaginary part of the surface dielectric function for O_2 adsorption at coverage $\theta = 1.2$.

region. We first show that these effects should be small and that they cannot explain the main features of the spectra.

The tails of extended states of the bulk undoubtedly penetrate into the surface region, so correct effective surface dielectric functions $\hat{\epsilon}^a$ and $\hat{\epsilon}^i$ are expected to include contributions of essentially the same form as the structures in $\hat{\epsilon}^b(\omega)$. Since the magnitude of this contribution could be somewhat different for the clean and adsorbate-covered surfaces, $\Delta\hat{\epsilon}^s(\omega)$ should in principle include a term $\Delta\hat{\epsilon}^b(\omega)$ proportional to $\hat{\epsilon}^b(\omega)$. Such effects cannot be the primary cause of the observed reflectance changes above 1.5 eV because one would then expect very similar $\Delta R/R(\hbar\omega)$ spectra for all adsorbates, contrary to observation. If $\Delta\hat{\epsilon}^b(\omega)$ were the dominant contribution to $\Delta\hat{\epsilon}^s(\omega)$, the oscillator expansion [Eq. (8)] which omits an explicit $\Delta\hat{\epsilon}^b(\omega)$ would produce a $\Delta\hat{\epsilon}^s(\omega)$ very similar to $\Delta\hat{\epsilon}^b(\omega)$ and therefore similar in shape to $\hat{\epsilon}^b(\omega)$. However, above 1.5 eV the structures in $\Delta\epsilon_2^s(\omega)$ (Figs. 10–12) bear no evident relation to those in $\epsilon_2^b(\omega)$. Thus chemisorption-induced changes in the bulk dielectric response within the surface region do not seem to play a significant role.

Below 1–1.5 eV, the oscillator strength of the metal is primarily Drude (intraband) in origin. Chemisorption should reduce the free-electron density and relaxation (scattering) time near the surface by tying up some of the electrons of the metal in the chemisorption bond and by causing strong scattering of conduction electrons by the adatoms. If adsorption-induced changes in the Drude oscillator strength at the surface dominated the reflectance changes, one would expect the reflectance to change continuously with coverage up to a full monolayer, contrary to observation. Furthermore, chemisorption-induced changes in a Drude contribution to $\Delta\epsilon_2^s$ at low $\hbar\omega$ should be too small to explain the large magnitude of $\Delta\epsilon_2^s$ at low $\hbar\omega$ (determined by the fitting procedure to about $\pm 30\%$). For the nominal 5 Å thickness assumed for the surface region, $|\Delta\epsilon_2^s| \gtrsim \epsilon_2^b$ at low $\hbar\omega$; if a slightly smaller but perhaps more reasonable thickness (~ 3.5 Å) were assumed, $|\Delta\epsilon_2^s|$ would be even larger. Even if the total $\Delta\epsilon_2^s$ were due solely to changes in the Drude response at the surface, the largest possible negative value of $\Delta\epsilon_2^b$ would be $-\epsilon_2^b$, which is smaller in magnitude than the required $\Delta\epsilon_2^s$. A reasonable estimate of the maximum value of $|\Delta\epsilon_2^b|$ near the surface is $\frac{1}{4}\epsilon_2^b$.⁴²

Thus we conclude that for both low and high $\hbar\omega$, significant contributions to $\Delta\epsilon_2^s(\hbar\omega)$ from adsorbate-induced changes in the bulk optical response near the surface are unlikely. We therefore neglect such effects and analyze the $\Delta\epsilon_2^s(\hbar\omega)$ spectra on the basis of optical excitations involving surface or-

bitals which are produced or quenched by chemisorption.

A. Structure below 1.5 eV: Intrinsic surface states

A strong dip in $\Delta\epsilon_2^s$ below $\hbar\omega = 1.5$ eV dominates the $\Delta\epsilon_2^s(\hbar\omega)$ spectra for all three adsorbates, as seen in Figs. 10–12, and gives rise to the strong structure at low $\hbar\omega$ observed in the $\Delta R/R(\hbar\omega)$ curves in Figs. 7–9. Because this structure is essentially independent of the adsorbate identity, it is most likely characteristic of the metal surface itself. Furthermore, since the structure is represented as a strong oscillator of negative amplitude, it must arise from a term in the dielectric function of the clean surface which is suppressed by adsorption, i.e., from strong surface optical transitions which are quenched by chemisorption of any of the adatom species studied here. Finally, we note that at low $\hbar\omega$ the magnitude of the dip in $\Delta\epsilon_2^s$ is approximately inversely proportional to coverage: for H₂ (Fig. 10), $\Delta\epsilon_2^s(\theta = 0.19) \cong 5\Delta\epsilon_2^s(\theta = 1.00)$ and for CO (Fig. 11), $\Delta\epsilon_2^s(\theta = 0.44) \cong 2\Delta\epsilon_2^s(\theta = 1.00)$. This decrease of $\Delta\epsilon_2^s$ with θ above the fractional coverages given arises not from a further physical change in surface electronic structure, but rather from the definition of a dielectric function as polarizability per unit volume. Thus after the changes in surface electronic structure and reflectance at low $\hbar\omega$ have saturated at the fractional coverage, the magnitudes of $\Delta\epsilon_1^s$ and $\Delta\epsilon_2^s$ must decrease with further coverage as the surface region thickness increases to keep $\Delta R/R$ constant. In contrast, if each additional adatom caused the same change in surface electronic structure for all coverage, $\Delta\hat{\epsilon}^s$ would be constant with θ and $\Delta R/R$ would increase linearly with d_a or θ .

We therefore attribute the prominent dip in $\Delta\epsilon_2^s(\hbar\omega)$ to adsorbate-induced quenching of strong optical excitations of filled intrinsic surface states of the clean W(100) surface.¹⁷ The position of these states, about 0.4 eV below the Fermi energy E_F , and their behavior with adsorption have been documented by both UPS^{2,3} and FES^{4,5} measurements. These surface states are quenched by the mere presence of adsorbates, as shown for H₂, CO, O₂, N₂ and C,⁴³ and as indicated by the results in Figs. 10–12. The saturation of reflectance changes near $\theta = 0.19$ for H₂ and $\theta = 0.44$ for CO adsorbates is in good agreement with the reported observations that H₂ coverage of $\theta = 0.2$ (Ref. 2) to 0.25 (Ref. 3) and CO coverage of $\theta = 0.4$ (Ref. 5) quenches the intrinsic surface states. Thus the slope discontinuity in the CO coverage curves (Fig. 5) at $\theta = 0.44$ for low $\hbar\omega$ signifies that quenching of the intrinsic surface states is complete, rather than that adsorption into a new binding configuration has begun.

Since a distinct structure is found in the $\Delta\epsilon_2^s(\hbar\omega)$

spectra, the filled surface states must be preferentially excited to a band of empty final states. Although the position and shape of the absorption band for these transitions cannot be very accurately determined (owing to the larger error bars at low $\hbar\omega$ and the assumed oscillator line shape of the structures), the transitions are concentrated below ~ 0.5 eV, so the final states for excitations from the surface states at -0.4 eV must lie at or just above E_F . These final states are most likely tails of extended states of the metal which may be modified somewhat at the surface from their form in the bulk. The strongly preferential coupling of the surface states to final states near E_F suggests that the strength of optical excitations of the intrinsic surface states decreases for higher-lying final states (increasing photon energy). This trend may explain why the photoemission yield of the surface states relative to bulk states decreases with increasing photon energy,² in contrast with the behavior expected from the usual energy-dependence of the hot electron attenuation length.

The large magnitude of the intrinsic surface state dip in $\Delta\epsilon_2^s$, of the order of ϵ_2^b for the tungsten substrate, implies that the surface states cause a significant modification of the electronic structure near the surface as seen at low $\hbar\omega$. In this region the oscillator strength of the bulk metal is primarily Drude (intraband) in character. If oscillator strength is assumed to be conserved locally, then it appears that near the surface of the clean metal a considerable portion of the Drude oscillator strength found in the bulk is shifted into intrinsic surface state excitations.

B. Structure above 1.5 eV: Adsorbate-induced surface orbitals

The structures in the $\Delta\epsilon_2^s(\hbar\omega)$ spectra (Figs. 10–12) above 1.5 eV differ with adsorbate identity and coverage and hence are characteristic of the particular adatom/surface atom chemisorption bond and binding configuration. These features appear as peaks which represent new adsorbate-induced optical transitions associated with the surface electronic structure. Table I lists the positions of these peaks in the $\Delta\epsilon_2^s(\hbar\omega)$ spectra for H_2 , CO, and O_2 adsorbates on W(100) as determined by SRS. Although one might expect similar or related transitions in electron-energy-loss spectra, such measurements for these systems have not yet shown clear evidence for adsorbate-induced loss peaks⁴⁴ for the adsorbates studied here. The interpretation of optical excitations from their transition energies (energy differences) can be greatly aided by comparison with electron spectroscopy results which give the absolute energy position of filled states. We therefore include in Table I the positions of filled adsorbate-induced surface orbitals (relative to E_F) as determined by UPS measure-

ments of various workers.

The energies of surface optical transitions determined by SRS show a marked correlation with the UPS results in Table I. For saturation coverage, the SRS transition energies for H_2 at 2.5 and near 5.0 eV, CO at 3.5 eV and a weaker structure near 2.4 eV, and O_2 at 4.5 eV match very well the position of filled UPS levels below the Fermi energy. This agreement suggests a simple interpretation—that these surface optical transitions are excitations from the filled adsorbate-induced surface orbitals seen by UPS to a common set of empty final states at or just above E_F ; for if final states at E_F are assumed, as appeared to be justified for the intrinsic surface state excitations at low $\hbar\omega$, the SRS transition energies then imply initial states which are in good agreement with the UPS results. For saturation coverage only the O_2 transition at 3.25 eV deviates from this pattern; if it is associated with the surface orbital at -2.5 or -2.0 eV, it indicates a final state ~ 1 eV above E_F , at about the position of a pronounced conduction-band threshold where the calculated density of states for tungsten rise sharply from small values near E_F .⁴⁵ The 2.2-eV transition for H_2 at $\theta \sim 0.2$ lies at an energy value between the UPS levels near -1.2 and -3.3 eV while the 3.0-eV CO transition at $\theta \sim 0.5$ lies between the -2 and -3.5 eV UPS levels. These results for intermediate coverages may also be consistent with the assumption of final states at E_F , since for lower θ the $\Delta R/R$ values are smaller and the resulting $\Delta\epsilon_2^s(\hbar\omega)$ spectra less accurate, so the peaks in $\Delta\epsilon_2^s(\hbar\omega)$ for intermediate coverage may represent some average of transitions from the UPS levels to E_F . Thus, we believe that the surface optical transitions above 1.5 eV determined by SRS very likely represent excitations from the filled adsorbate-induced surface orbitals seen by UPS to empty final states at or just above the Fermi energy which are probably the tails of extended states of the bulk as modified near the surface.

VII. CONCLUSIONS

Correlation of the SRS transition energies with UPS data for H_2 , CO, and O_2 chemisorption on W(100) gives the strong indication that optical excitations from intrinsic surface states and adsorbate-induced surface orbitals lying an energy E_s below the Fermi energy involve final (empty) states concentrated primarily at the Fermi energy. Structure in the optical constants might be expected near $\hbar\omega = E_s$ since the cutoff in the Fermi-Dirac distribution function at E_F produces an edge in $\Delta\epsilon_2^s(\hbar\omega)$ when the photon energy is just large enough to excite electrons from peaks in the density of filled surface states to the lowest empty states, which are at E_f . Such an edge occurs even for

TABLE I. Surface optical transition energies from SRS (present work) and energy levels of filled surface orbitals (relative to E_F) from UPS measurements for H_2 , CO, and O_2 chemisorption at various coverages.

Adsorbate	θ (monolayers)	SRS transition energies (eV)	UPS energy levels (eV)		
H_2	~ 0.2	2.2 ± 0.3	-1.15^a	-1.2^b	-1.1^c
			-3.2^a	-3.6^b	-3^c
			-5.5^a	-5.7^b	-5.4^c
	1.0	2.5 ± 0.1 5.0 ± 0.3	-2.4^a	-2^b	-2.4^c
			-5.0^a	-4.7^b	
CO	~ 0.5	3.0 ± 0.2	-2^d		
			-3.5^d		
			-5.9^d (unordered)		
	1.0	2.4 ± 0.4 3.5 ± 0.2	-2.5^e	-2^d	
			-3.5^e	-3.5^d	
				-6.0^d	
		-8.9^d			
O_2	~ 1.2	3.25 ± 0.2 4.5 ± 0.4	-2.5^e	-2.0^a	
			-4.5^f	-4.9^a	
			-6.5^e	-6.4^a	

^aReference 25.

^bReference 26.

^cReference 27.

^dReference 35.

^eReference 2.

^fReference 43.

constant matrix elements and a flat density of empty states above E_F , and is accentuated (especially at low $\hbar\omega$) by the $1/\omega$ factor in the imaginary part of the dielectric function. The resulting peak in $\Delta\epsilon_2^s(\hbar\omega)$ would be shifted above $\hbar\omega = E_s$ by about half the width of the peak in the filled density of states and broadened considerably (by a factor of 2 or more). However, the SRS spectral features (as seen in Fig. 7, for example) are not significantly broader than the surface-orbital peaks seen in UPS, and the correlation of SRS transition energies with the position of filled surface orbitals relative to E_F as seen in UPS is considerable. This suggests that optical excitations of electrons in the filled surface orbitals may in fact be enhanced by oscillator strength and/or joint-density-of-states effects for final states close to E_F . Detailed analysis of SRS spectra for a variety of chemisorption systems is needed to more fully understand the SRS line shapes.

Since the results can be interpreted in a simple way consistent with the UPS data by assuming common final states at E_F , these measurements give no firm evidence for significant empty surface orbitals. This is somewhat as expected since the primary candidates for such states—the excited states and affinity levels of the adsorbed species—lie considerably above E_F (by at least 4 eV)⁴¹ and are therefore nearly inaccessible in our spectral region ($\hbar\omega < 4.8$ eV). However, the possible ex-

istence and observation of empty surface orbitals in other systems, especially for adsorbates with low-lying excited states, remains an open question.

Similarly, the ground-state energy levels of the adsorbates studied here should be too far below E_F (~ 6 eV) to be excited in our measurements.^{41, 46} The adsorbate-induced surface orbitals for which optical excitations have been deduced by SRS are thought to be states derived primarily from the d electrons of the surface tungsten atoms within the molecular complex⁴¹ created by the chemisorption bond at the surface.^{26, 43, 47} However, the 5.0-eV transition for H_2 at saturation corresponds to the lowest-lying adsorbate level reported from UPS studies, so it is possible that this level involves a fairly strong admixture of the H(1s) ground state and the low-lying tungsten d states, as in the case of the Pd/H system.⁴⁸

The dielectric model of McIntyre and Aspnes which we have used to deduce spectroscopic information from the observed $\Delta R/R$ admittedly oversimplifies the relation between the measured reflectance changes and the actual electronic structure near the surface. If a local dielectric response can in fact be assumed and properly defined, it certainly changes with depth into the surface, and its depth dependence very likely varies with photon energy. However, by representing these complicated effects by a single effective complex dielec-

tric function averaged over the surface region and relating the surface-layer thickness to coverage in a simple way, the number of parameters characterizing the dielectric response of the surface is greatly reduced. As a result, valuable information can be extracted from experiment to give insight into the surface electronic structure through its optical excitations. The agreement between the SRS and UPS results obtained using a simple

interpretation of the optical transitions (single band of final states at E_F) can be viewed as reassuring evidence that the dielectric model employed here is physically meaningful.

ACKNOWLEDGMENTS

We appreciate stimulating and helpful discussions with D. E. Eastman, E. W. Plummer, P. J. Estrup, and J. D. E. McIntyre.

*Supported in part by the Army Research Office, Durham, N. C., and by the National Science Foundation through the Materials Science Program at Brown University.

†Present address: Dept. of Physics, Montana State University, Bozeman, Mont. 59715.

‡Part of this work was carried out at Brown University.

¹D. E. Eastman and J. K. Cashion, *Phys. Rev. Lett.* **27**, 1520 (1971).

²B. J. Waclawski and E. W. Plummer, *Phys. Rev. Lett.* **29**, 783 (1972).

³B. Feuerbacher and B. Fitton, *Phys. Rev. Lett.* **29**, 786 (1972).

⁴E. W. Plummer and J. W. Gadzuk, *Phys. Rev. Lett.* **25**, 1493 (1970).

⁵P. L. Young and R. Gomer, *Phys. Rev. Lett.* **30**, 955 (1973).

⁶H. D. Hagstrum and G. E. Becker, *Phys. Rev. Lett.* **22**, 1054 (1969); *J. Chem. Phys.* **54**, 1015 (1971).

⁷J. E. Rowe and H. Ibach, *Phys. Rev. Lett.* **31**, 102 (1973).

⁸F. Steinrisser and E. N. Sickafus, *Phys. Rev. Lett.* **27**, 992 (1971); *Phys. Rev. B* **6**, 3714 (1972).

⁹J. D. E. McIntyre, *Surf. Sci.* **37**, 658 (1973).

¹⁰J. D. E. McIntyre, *Advances in Electrochemistry and Electrochemical Engineering*, edited by R. H. Muller (Wiley, New York, 1973), Vol. 9, p. 61.

¹¹G. Chiarotti *et al.*, *Phys. Rev. B* **4**, 3398 (1971).

¹²J. J. Carroll and A. J. Melmed, *Surf. Sci.* **16**, 251 (1969).

¹³F. Meyer, E. E. De Kluzenaar, and G. A. Bootsma, *Surf. Sci.* **27**, 88 (1971).

¹⁴F. Meyer, *Phys. Rev. B* **9**, 3622 (1974).

¹⁵J. Anderson, G. W. Rubloff, and P. J. Stiles, *Solid State Commun.* **12**, 825 (1973).

¹⁶G. W. Rubloff, J. Anderson, and P. J. Stiles, *Surf. Sci.* **37**, 75 (1973).

¹⁷G. W. Rubloff, J. Anderson, M. A. Passler, and P. J. Stiles, *Phys. Rev. Lett.* **32**, 667 (1974).

¹⁸P. J. Estrup and J. Anderson, *J. Chem. Phys.* **45**, 2254 (1966).

¹⁹U. Gerhardt and G. W. Rubloff, *Appl. Opt.* **8**, 305 (1969).

²⁰T. E. Madey, *Surf. Sci.* **36**, 281 (1973).

²¹P. W. Tamm and L. D. Schmidt, *J. Chem. Phys.* **54**, 4775 (1971).

²²D. L. Adams and L. H. Germer, *Surf. Sci.* **23**, 419 (1970).

²³E. W. Plummer and A. E. Bell, *J. Vac. Sci. Technol.* **9**, 583 (1972).

²⁴J. Anderson, G. W. Rubloff, M. A. Passler, and P. J. Stiles, *J. Vac. Sci. Technol.* **11**, 271 (1974).

²⁵D. E. Eastman, J. M. Baker, and J. E. Demuth, in

Proceedings of the European Physical Society Conference on Metal Surfaces, Hindas, Sweden, 1973 (unpublished).

²⁶E. W. Plummer, in Ref. 25.

²⁷B. Feuerbacher and B. Fitton, *Phys. Rev. B* **8**, 4890 (1973).

²⁸J. Anderson and P. J. Estrup, *J. Chem. Phys.* **46**, 563 (1967).

²⁹L. R. Clavenna and L. D. Schmidt, *Surf. Sci.* **33**, 11 (1972).

³⁰J. T. Yates, Jr. and D. A. King, *Surf. Sci.* **32**, 479 (1972).

³¹R. A. Armstrong, *Can. J. Phys.* **46**, 949 (1968).

³²T. E. Madey, *Surf. Sci.* **33**, 355 (1972).

³³P. J. Estrup and J. Anderson, Proceedings of the Annual Physical Electronics Conference, MIT, 1967 (unpublished).

³⁴Yu. G. Ptushinskii and B. A. Chuikov, *Fiz. Tverd. Tela* **10**, 722 (1968) [*Sov. Phys. -Solid State* **10**, 565 (1968)].

³⁵J. M. Baker and D. E. Eastman, *J. Vac. Sci. Technol.* **10**, 223 (1973).

³⁶J. D. E. McIntyre and D. E. Aspnes, *Surf. Sci.* **24**, 417 (1971).

³⁷J. J. Carroll and A. J. Melmed, *J. Opt. Soc. Am.* **61**, 470 (1971); D. W. Juenker, L. J. LeBlanc, and C. R. Martin, *ibid.* **58**, 164 (1968); S. Roberts, *Phys. Rev.* **114**, 104 (1959).

³⁸See, e.g., W. J. Scouler and P. M. Raccach, *Bull. Am. Phys. Soc.* **15**, 289 (1970); H. W. Verleur, *J. Opt. Soc. Am.* **58**, 1356 (1968).

³⁹P. W. Anderson, *Phys. Rev.* **124**, 41 (1961).

⁴⁰J. R. Schrieffer, *J. Vac. Sci. Technol.* **9**, 561 (1972); D. M. News, *Phys. Rev.* **178**, 1123 (1969).

⁴¹T. B. Grimley, in *Molecular Processes on Solid Surfaces*, edited by E. Drauglis, R. D. Gritz, and R. I. Jaffee (McGraw-Hill, New York, 1969), p. 299.

⁴²A maximum value of $|\Delta\epsilon_2^D|$ for Drude effects near the surface may be estimated as follows. The Drude contribution to ϵ_2 is $\omega_p^2/[\omega\tau(\omega^2 + \tau^{-2})]$. Near $\hbar\omega = 0.5$ eV, $\omega\tau = 1$. Chemisorption bonds for a full monolayer of H_2 (two H atoms per surface W atom) could tie up two of the six conduction electrons per surface W atom; if only the surface W atoms contribute to the surface region, then the electron density N and the square of the plasma frequency $\omega_p^2 = 4\pi Ne^2/m$ would decrease by the factor $\frac{2}{3}$. The relaxation time for the conduction electrons at the surface might also decrease by a factor of 2, so $1/(\omega^2 + \tau^{-2})$ could decrease by the factor $\frac{2}{5}$. As a result $|\Delta\epsilon_2^D|$ near the surface could be at most $\frac{2}{3} \times \frac{2}{5} = \frac{4}{15}$ or about $\frac{1}{4}$ of ϵ_2^D .

⁴³B. J. Waclawski and E. W. Plummer, *J. Vac. Sci. Technol.* **10**, 292 (1973).

⁴⁴D. E. Edwards, Jr. and F. M. Propst, *J. Chem. Phys.*

- 55, 5175 (1971).
- ⁴⁵L. F. Mattheis, Phys. Rev. 139, A1893 (1965); I. Petroff and C. R. Viswanathan, *Proceedings of the Electronic Density of States Conference, Gaithersburg, Md.*, 1969, Natl. Bur. Stds. Publ. No. 323 (U. S. GPO, Washington, D. C., 1971), p. 53.
- ⁴⁶The levels derived primarily from the ground-state orbitals of the adsorbate are thought to be (see references in Table I) -5.9 and -6.1 eV for β CO at $\theta=1.0$; -8.9 eV for α CO at $\theta=1.0$; ~ -6.0 eV for O₂ at $\theta \sim 0.5$; ~ -6.5 eV for O₂ at $\theta=1.0$; and possibly the H₂ levels at -5.5 eV for $\theta \sim 0.2$ and at -5 eV for $\theta=1.0$.
- ⁴⁷D. E. Eastman, J. E. Demuth, and J. M. Baker, J. Vac. Sci. Technol. 11, 273 (1974).
- ⁴⁸D. E. Eastman, J. K. Cashion, and A. C. Switendick, Phys. Rev. Lett. 27, 35 (1971).